

Mussel-Inspired Polydopamine Coating as a Universal Route to Hydroxyapatite Crystallization

By Jungki Ryu, Sook Hee Ku, Haeshin Lee,* and Chan Beum Park*

Bone tissue is a complex biocomposite material with a variety of organic (e.g., proteins, cells) and inorganic (e.g., hydroxyapatite crystals) components hierarchically organized with nano/microscale precision. Based on the understanding of such hierarchical organization of bone tissue and its unique mechanical properties, efforts are being made to mimic these organic–inorganic hybrid biocomposites. A key factor for the successful designing of complex, hybrid biomaterials is the facilitation and control of adhesion at the interfaces, as many current synthetic biomaterials are inert, lacking interfacial bioactivity. In this regard, researchers have focused on controlling the interface by surface modifications, but the development of a simple, unified way to biofunctionalize diverse organic and inorganic materials remains a critical challenge. Here, a universal biomineralization route, called polydopamine-assisted hydroxyapatite formation (pHAF), that can be applied to virtually any type and morphology of scaffold materials is demonstrated. Inspired by the adhesion mechanism of mussels, the pHAF method can readily integrate hydroxyapatites on ceramics, noble metals, semiconductors, and synthetic polymers, irrespective of their size and morphology (e.g., porosity and shape). Surface-anchored catecholamine moieties in polydopamine enriches the interface with calcium ions, facilitating the formation of hydroxyapatite crystals that are aligned to the *c*-axes, parallel to the polydopamine layer as observed in natural hydroxyapatites in mineralized tissues. This universal surface biomineralization can be an innovative foundation for future tissue engineering.

formation of skeletal frames.^[1] For example, the fascinating chemical and mechanical properties of natural bone originate from its controlled hierarchical structure in which hydroxyapatite, a calcium phosphate (CaP) crystal with a formula of $\text{Ca}_{10}(\text{PO}_4)_6(\text{OH})_2$, is formed and spatially aligned between collagen fibrils.^[2] Over the last two decades, researchers have focused on understanding the mechanism of biomineralization in natural systems^[3] and attempted to mimic the biomineralization phenomena.^[4] However, none of the previous studies have offered a practical and generalized methodology that can integrate natural inorganic crystals (e.g., hydroxyapatite) into a wide variety of synthetic materials to create the next generation of hybrid biomaterials. Unlike natural organic materials, such as collagen, sialoprotein, and osteonectin, that nucleate and align hydroxyapatite crystals, thus forming overall shapes with cell-adhesive moieties,^[3] the bio-inertness and non-bioactivity found in current synthetic biomaterials are a significant hurdle for the successful fabrication of novel biomaterials.^[5] Therefore, the design of biointerfaces, through which natural components can be readily inte-

grated into diverse synthetic biomaterials, remains a key challenge in chemistry, materials science, and tissue engineering.

Inspired by mussel-adhesion phenomena in nature,^[6] we report herein a universal biomineralization route that can integrate inorganic hydroxyapatite crystals within versatile materials. This is a simple, aqueous, two-step functionalization approach, called polydopamine-assisted hydroxyapatite formation (pHAF), that consists of i) the chemical activation of material surfaces via polydopamine coating and ii) the growth of hydroxyapatite in a simulated body fluid (SBF or Kokubo solution^[7]) (Fig. 1a). Polydopamine is a mimic of the specialized adhesive foot protein, Mefp-5 (Mytilus edulis foot protein-5),^[6a] in which the catechol moiety strongly binds to various metal ions.^[8] This indicates the possibility of hydroxyapatite formation by co-precipitation of calcium and phosphate ions. Indeed, we have found that pHAF is a powerful approach to create hydroxyapatite-based, novel organic–inorganic hybrid biomaterials regardless of type, size, and shape of hybridized counterpart materials.

1. Introduction

The molecular arrangement of organic and inorganic components into hierarchically well-organized composite materials is one of the most important biochemical phenomena in the

[*] Prof. C. B. Park, J. Ryu, S. H. Ku
Department of Materials Science and Engineering
KAIST Institute for the BioCentury (KIB) and the NanoCentury (KINC)
Korea Advanced Institute of Science and Technology (KAIST)
335 Science Road, Daejeon 305-701 (Republic of Korea)
E-mail: parkcb@kaist.ac.kr
Prof. H. Lee
Department of Chemistry, Molecular-Level Interface Research Center
KAIST Institute for the BioCentury (KIB) and the NanoCentury (KINC)
Korea Advanced Institute of Science and Technology (KAIST)
335 Science Road, Daejeon 305-701 (Republic of Korea)
E-mail: haeshin@kaist.ac.kr

DOI: 10.1002/adfm.200902347

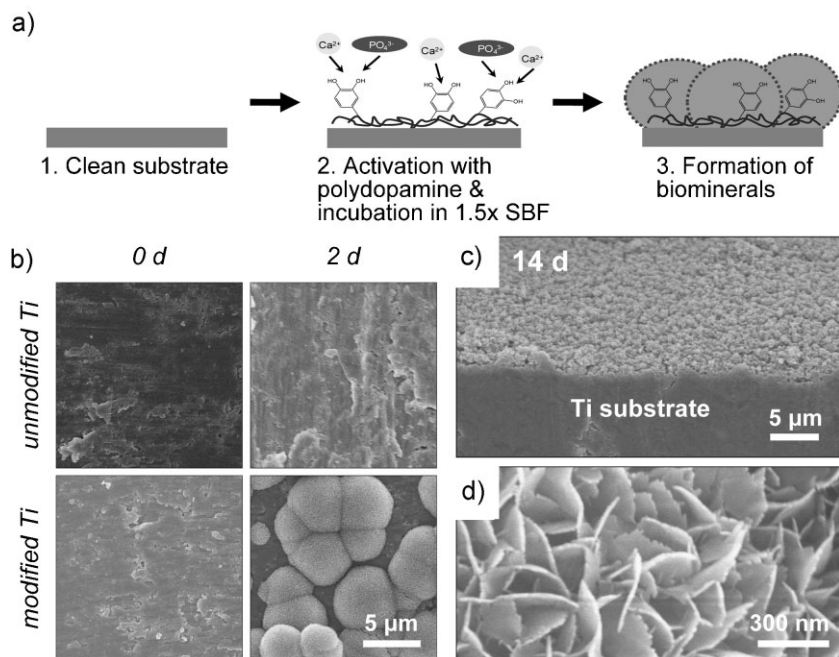


Figure 1. The formation of calcium phosphate biominerals facilitated by polydopamine, a catecholamine, inspired by the adhesion mechanisms of mussels. a) Scheme for polydopamine-assisted calcium phosphate crystal formation. b) Electron microscopy images showing the effect of polydopamine modification of the Ti substrate on the formation of calcium phosphate minerals. c,d) After incubation for 2 weeks: c) the entire surface of polydopamine-coated Ti was uniformly covered with calcium phosphate minerals, and d) a lath-like structure, typically found in natural hydroxyapatite crystals, was observed by high-magnification SEM.

2. Results and Discussion

Polydopamine-coated substrates were prepared by the simple immersion of the substrates in an aqueous solution of dopamine (2 mg mL^{-1} in 10 mM Tris buffer, pH 8.5, see Experimental), and the substrate was transferred to $1.5\times$ SBF for biomineralization. First, we tested titanium (Ti) substrates that have been widely utilized for load-bearing orthopedic applications because of their unique mechanical properties and corrosion resistance.^[9] As shown in Figure 1, the polydopamine coating rapidly facilitated CaP nucleation. The polydopamine-coated Ti substrate, for instance, began to form hemispherical CaP agglomerates after just 1 day of incubation, and the agglomerates covered most of the surface area in 2 days (Fig. 1b). Note that the nucleation of CaP began when the polydopamine layer was thicker than 40 nm (Fig. S1 in the Supporting Information), which implies that the amount of free catechols not participating in substrate adhesion is important for CaP nucleation. After incubation for two weeks the Ti substrate was fully and uniformly covered by CaP minerals (Fig. 1c), whereas the unmodified substrate did not show such minerals even after incubation for two weeks. High-magnification scanning electron microscopy (SEM) images reveal that the agglomerates have a lath-like structure, a typical form for hydroxyapatite crystals (Fig. 1d). According to energy dispersive X-ray (EDX) analysis, the Ca/P ratio for the CaP agglomerates was 1.65, which is close to the theoretical ratio of hydroxyapatite (Ca/P = 1.67) (Fig. S2). EDX mapping analysis clearly showed that Ca and P are predominantly distributed along the inorganic

aggregates (Fig. S2a and S2c). In contrast, only trace amounts of Ca (0.07%) and P (0.25%) elements were measured in the regions without agglomerates (Fig. S2a and S2b). The observed morphological change suggests that the formation of CaP biominerals on the polydopamine-coated surface follows a layer-by-layer growth mode by strong interactions between polydopamine and biominerals rather than other growth modes such as island or layer-plus-island growth mode (Fig. S3).^[10] Our results suggest that the abundant catecholamine moieties in polydopamine play a dual role; namely, that of molecular anchor for a wide range of substrates (catecholamines located at the interfaces are involved in this) and that of Ca^{2+} ion binder (catecholamines not participating in substrate adhesion), as evidenced by X-ray photoelectron spectroscopy (XPS) analysis (Fig. 2).

We applied multiple analytical tools to characterize the structure of the CaP agglomerates produced by pHAF. Transmission electron microscopy (TEM) analysis revealed that the inorganic agglomerates consisted of plate-like nanocrystals (Figs. 3a and S4). Electron diffraction (Fig. 3b) and EDX (Fig. 3c) analysis confirmed that the plate-shaped nanocrystals were hydroxyapatite. The diffraction pattern of the CaP agglomerates grown directly in contact with polydopamine exhibited diffraction arcs

corresponding to the (002) and (004) planes, implying that polydopamine guides the directional growth of hydroxyapatite crystals aligned with their *c*-axes parallel to polydopamine.^[4e] X-ray diffraction analysis also proved that the mineral grown on the surface was hydroxyapatite rather than octacalcium phosphate, which is structurally similar to hydroxyapatite^[4i] (Figs. 3d and 4). Note that the broad peak is related to its nanocrystalline nature. The formation of hydroxyapatite onto the polydopamine-coated Ti substrate was further investigated by Raman spectroscopy (Fig. 3e). Before the growth of hydroxyapatite, the polydopamine-coated Ti surface exhibited two broad peaks at 1370 and 1630 cm^{-1} , corresponding to the stretching and deformation of the catechols, respectively.^[11] After 2 days, several new peaks appeared: the P-O vibration at 429 cm^{-1} , the O-P-O vibration at 593 cm^{-1} , and the P-O stretching vibration at 962 cm^{-1} .^[4b,12] In particular, the strongest peak at 962 cm^{-1} is a representative indication of crystalline hydroxyapatite.^[4b,12] A shoulder appeared at 1070 cm^{-1} that is attributed to CO_3^{2-} , implying that trace amounts of PO_4^{3-} were substituted by CO_3^{2-} .^[12] We further confirmed this partial substitution of PO_4^{3-} by CO_3^{2-} using Fourier-transform infrared (FTIR) spectroscopy^[13] (Fig. 5).

Using this pHAF approach, hydroxyapatite can be integrated within any material with extreme ease. We attempted the modification of various materials surfaces, such as metals (Ti, stainless steel, Si, Au), ceramics (SiO_2), semiconductors (Si_3N_4), and polymers (polystyrene (PS), poly(methyl methacrylate) (PMMA), poly(dimethylsiloxane) (PDMS), cellulose, polyester, nylon, and polytetrafluoroethylene (PTFE)) through

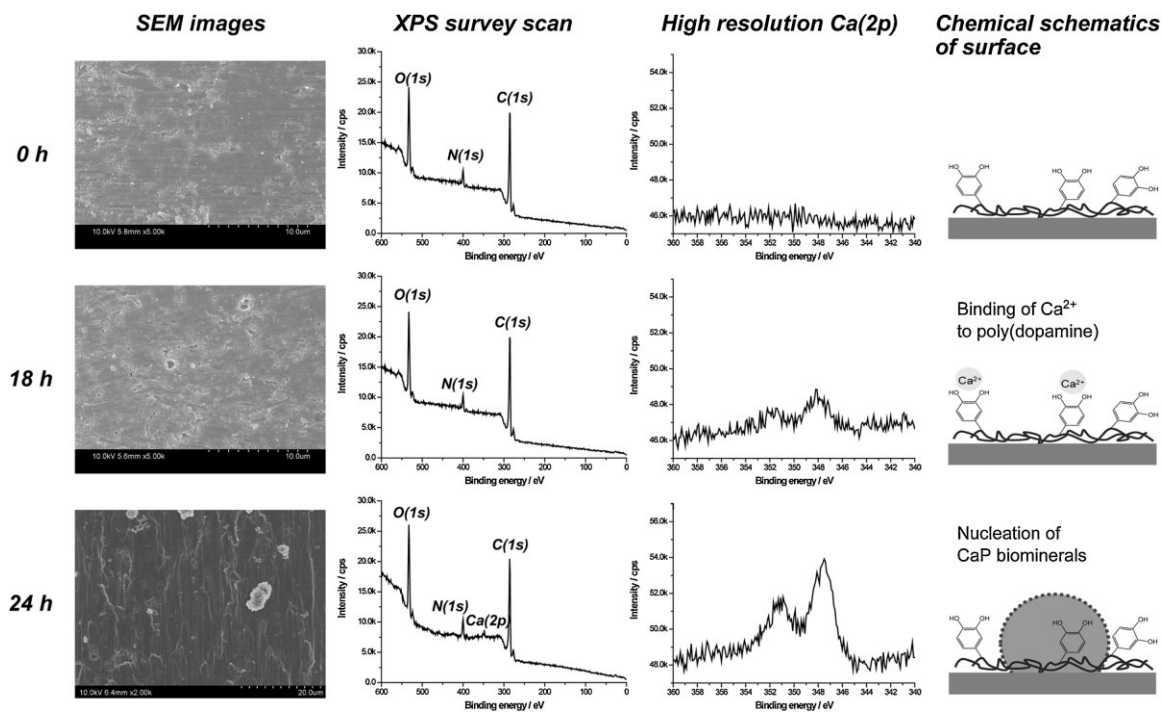


Figure 2. Surface analysis by XPS demonstrates that polydopamine binds to the Ca^{2+} ions, facilitating the formation of hydroxyapatites. A Ti substrate was coated with polydopamine by immersing the substrate in 2 mg mL^{-1} dopamine hydrochloride solution (10 mM Tris, pH 8.5) for 16 h. The polydopamine-coated substrates exhibited C(1s), N(1s), and O(1s) peaks without a substrate peak (i.e., Ti(2p)). After incubation for 18 h, a weak yet detectable Ca(2p) peak was observed without any indication of calcium phosphate mineral formation. This indicates that the Ca^{2+} ions bound in the polydopamine layers at an early stage facilitate the formation of calcium phosphate agglomerates later (24 h, bottom row).

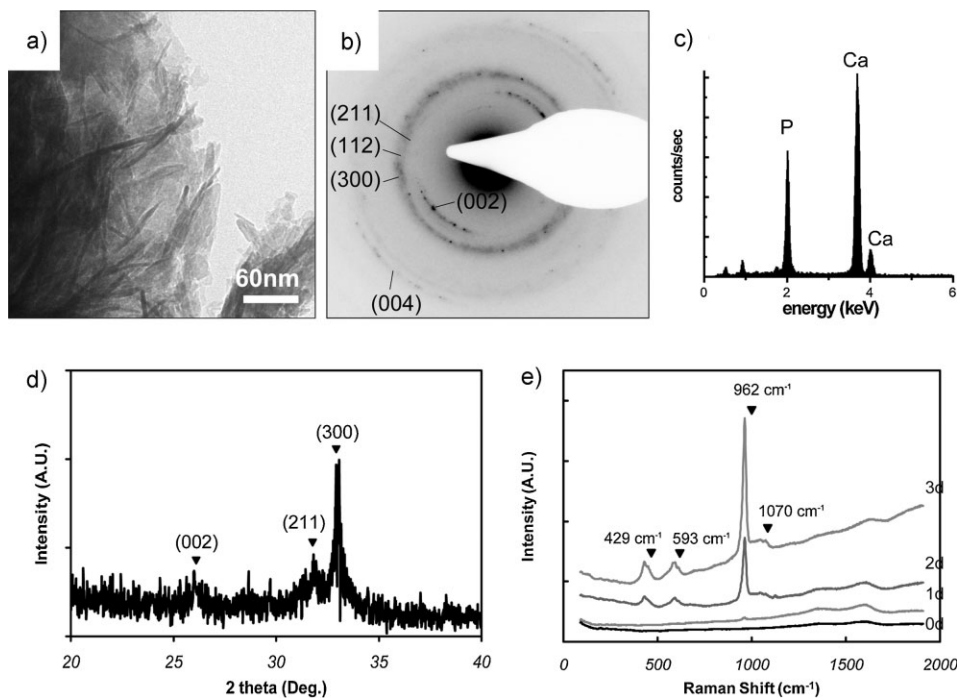


Figure 3. a–d) Structural analysis shows that the calcium phosphate agglomerates are hydroxyapatite crystals. a) TEM, b) SAED, c) EDX, and d) X-ray diffraction show a consistent indication of hydroxyapatite growth on the polydopamine-coated Ti substrate. e) The growth of hydroxyapatite on the polydopamine surface was further investigated by Raman spectroscopy. Raman peaks at $1370/1630 \text{ cm}^{-1}$ and $429/593/962 \text{ cm}^{-1}$ indicate the formation of polydopamine and hydroxyapatite crystals, respectively.

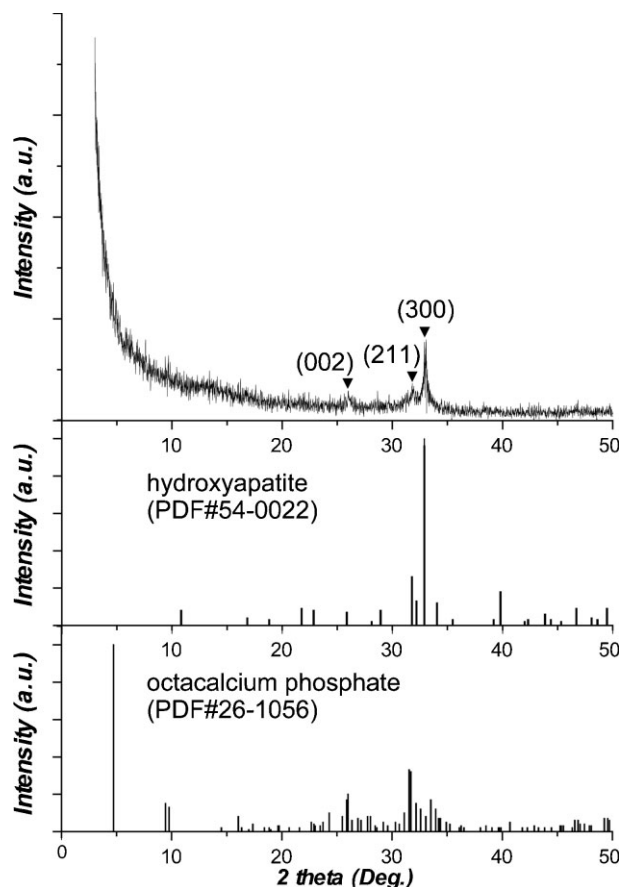


Figure 4. X-ray diffraction pattern of calcium phosphate minerals grown by the pHAF approach. The documented X-ray diffraction patterns of hydroxyapatite (PDF#54-0022) and octacalcium phosphate (PDF#26-1056) are shown for comparison, which suggest that the calcium phosphate minerals grown by pHAF are hydroxyapatite rather than octacalcium phosphate.

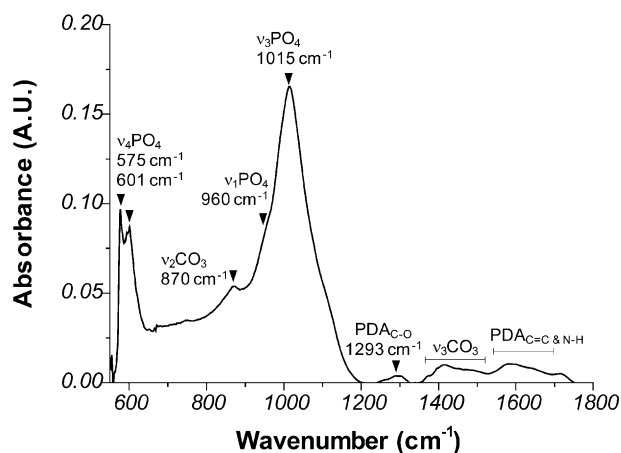


Figure 5. Fourier-transform infrared spectrum showing that the calcium phosphate minerals grown by pHAF are carbonated hydroxyapatite [13], similar to the natural bone hydroxyapatite. For the experiment, we incubated the polydopamine (PDA)-coated Ti substrate in $1.5\times$ SBF for 2 days at 37°C and analyzed it using a Hyperion 3000 spectrometer (Bruker Optics Inc., Germany) in an attenuated total reflection mode with a Ge single crystal at a resolution of 2 cm^{-1} .

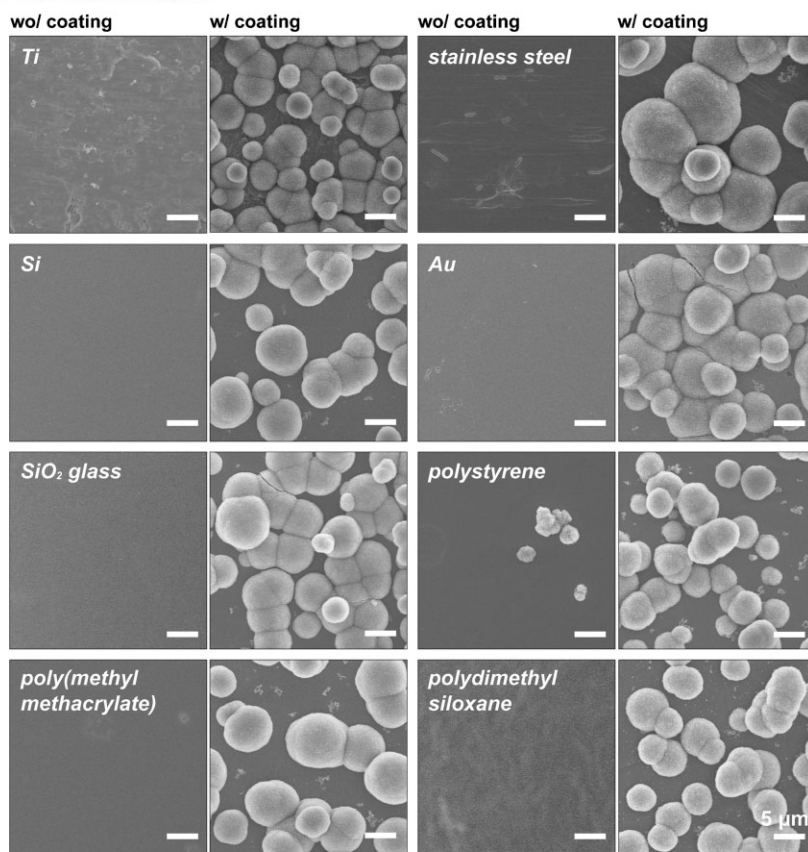
polydopamine coating. We found that the pHAF approach works universally for the growth of hydroxyapatite crystals regardless of the material type and morphology (Figs. 6 and 7). We also found that hydroxyapatite was efficiently generated on the surface of a microfabricated atomic force microscopy (AFM) cantilever (Si_3N_4), suggesting the geometrical versatility of the pHAF approach (Fig. 6b). The versatile applicability of the pHAF approach is a critical prerequisite for successful bone tissue engineering because of the intrinsic organic–inorganic hybrid nature of engineered bone tissue. In the case of Si substrates, the polydopamine layer was delaminated in the process of hydroxyapatite formation, but this problem was overcome by high-temperature curing at 150°C (Fig. S5).

Unlike gas-phase deposition of materials, the modification with polydopamine is based on a dip-coating process that can modify the inner surface of 3D porous materials. Therefore, in principle, hydroxyapatite crystals generated by the pHAF approach could be integrated within porous materials. Consequently, as expected, we were able to fully integrate hydroxyapatites into the pores of a variety of 3D materials, such as porous cellulose, polyester fibers, porous nylon, and PTFE membranes (Fig. 7). In contrast, the formation of hydroxyapatite was not observed on unmodified materials. The cross-section of the porous nylon shows that hydroxyapatites were grown inside the membrane (Fig. 7f). pHAF could also readily induce the formation of hydroxyapatite even on a popular, strong anti-adhesive material such as PTFE (Fig. 7h), demonstrating the practical potential of the pHAF approach.

We further investigated the cellular response on the polydopamine layer since the direct contact of cells with the coating would be unavoidable in tissue engineering. To test the toxicity of polydopamine, preosteoblasts were cultured on polydopamine layers. In-vitro viability tests and morphological observations showed no significant difference, indicating that polydopamine modification is non-toxic (Fig. S6). It is noteworthy that the polydopamine coating facilitates the attachment and proliferation of the cells independent of the underlying substrate, including for well-known anti-adhesive materials, such as PTFE and polydimethylsiloxane (PDMS). Recently, we have reported that the surface energy of polydopamine is a suitable platform for structurally intact cell surface adhesive proteins to be strongly adhered on surfaces.^[14]

The mechanical stability of the coating layer is critical for practical applications. We investigated the adhesion stability of the polydopamine layer using ultrasonication and peeling tests. The hydroxyapatite on the polydopamine coating remained stable after strong ultrasonication (42 kHz, 135 W) for 1 h; 83.1% of the hydroxyapatite was still firmly attached to the underlying Ti substrate (Fig. 8). Furthermore, we found that 85.4% of the hydroxyapatite remained after the peeling test utilizing a commercial adhesive, Scotch tape (KST1046), having an adhesive strength higher than 1.23 N cm^{-1} (Fig. 9). A number of recent reports demonstrated the good interfacial stability of polydopamine under various conditions.^[6] For example, polydopamine-modification was found to be useful as an anti-corrosive lubricant coating,^[6h,6i] and a single-molecule adhesion study revealed that the catechol–Ti adhesion force was four times stronger than biotin–streptavidin interactions.^[6j] These results suggest that polydopamine can work as an on-demand robust glue for creating functional biomaterials.

a) flat solid substrate



b) microfabricated Si₃N₄ cantilever

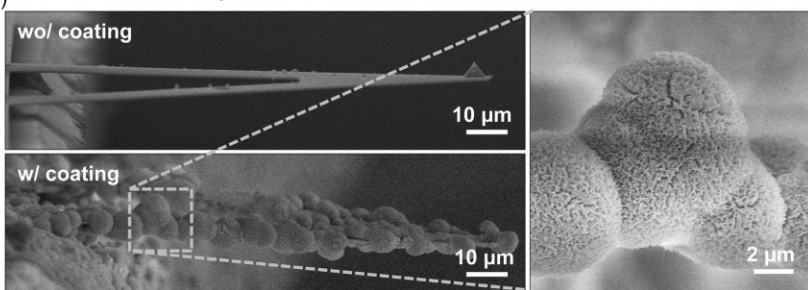


Figure 6. a) Material-independent hydroxyapatite formation via pHAF. The SEM images show that hydroxyapatites can cover any material surfaces by the enrichment of calcium ions on the polydopamine-coated surfaces. Hydroxyapatite was created on a wide range of flat solid substrates: noble metal and metal oxides [e.g., Ti, stainless steel (SUS 316L), Si, Au], ceramics (e.g., SiO₂ glass), and polymers [polystyrene, poly(methyl methacrylate), polydimethylsiloxane]. The scale bar represents 5 μm. b) An example of hydroxyapatite formation on a semiconducting material of a silicon nitride (Si₃N₄) atomic force microscope cantilever.

3. Conclusion

To date, the lack of bioactivity in current synthetic materials and the absence of universal biofunctionalization method have limited the choice of materials, slowing down the development of next generation biomaterials. In this report, we have demonstrated that the biomimetic, mussel-inspired pHAF approach can be a general

platform to create novel biomaterials by hybridizing any type and shape of synthetic biomaterials with natural inorganic crystals, hydroxyapatite. We found that catecholamine moieties that are abundant in polydopamine are responsible not only for the chemical functionalization of a wide range of material surfaces, but also for the nucleation of hydroxyapatite by concentrating Ca²⁺ ions at the interface. As the entire pHAF approach is a dip-coating process, we were able to integrate hydroxyapatites into virtually any morphology of materials. Enabling the directional *c*-axis growth of hydroxyapatite crystals upon the polydopamine film, a phenomenon that is the same as that found in the natural growth of biominerals, the pHAF approach can be a promising platform for the future development of advanced mineralized biomaterials.

4. Experimental

Substrate Preparation: Ti foil (0.25 mm thick, Sigma, MO, USA), stainless steel 316L (SUS-316L) foil (0.1 mm thick, Nilaco Corp., Japan), Si (p-type, TASCOS Ltd., Korea), gold, glass (Fisher scientific), poly(styrene) (211kDa, Sigma), poly(methyl methacrylate) (120kDa, Sigma), polydimethylsiloxane (PDMS, Sylgard 184, Dow Corning), microfabricated Si₃N₄ AFM cantilever (Veeco Instruments, NY, U.S.A.), filter paper (Whatman PLC, UK), nylon membrane filter (0.2 μm pore size, Whatman PLC, UK), and polytetrafluoroethylene (PTFE) membrane filter (0.2 μm pore size, Whatman PLC, UK) were all cleaned ultrasonically in 2-propanol before use. A gold (50nm deposited onto 10nm Cr) surface was prepared by electron-beam deposition on Si wafers. Poly(styrene) (PS) and poly(methyl methacrylate) (PMMA) films were prepared by spin-coating using a 1 wt% polymer solution in toluene (at 3000 rpm for 60 s), followed by curing at 100 °C. PDMS elastomer was prepared by mixing a precursor and a curing agent with a weight ratio of 10:1 followed by thermal curing at 60 °C.

Polydopamine-Assisted Hydroxyapatite Formation: This procedure was carried out as described by Lee and his colleagues [6a]. Briefly, a thin polydopamine layer was created onto the surface of any material by oxidative polymerization of dopamine-hydrochloride dissolved in 10 mM Tris buffer and the pH was adjusted to 8.5. The polydopamine coating was carried out for 16 h, unless a different coating time was mentioned. In order to modify the inside surfaces of nano- or microporous materials, the coating solution was applied using a vacuum pump. After coating for a desired time, polydopamine-coated substrates were

extensively rinsed with deionized water and dried with a stream of N₂ gas. The substrate coated with polydopamine was transferred into 1.5× simulated body fluid (SBF) and incubated at 37 °C to grow hydroxyapatite. The composition of 1.5× SBF was as follows: Na⁺, 213.0; K⁺, 7.5; Mg²⁺, 2.25; Ca²⁺, 3.75; Cl⁻, 221.7; HCO₃⁻, 6.3; HPO₄²⁻, 1.5; SO₄²⁻, 0.75 mM. Before characterization, each sample was rinsed with deionized water and dried with N₂ gas.

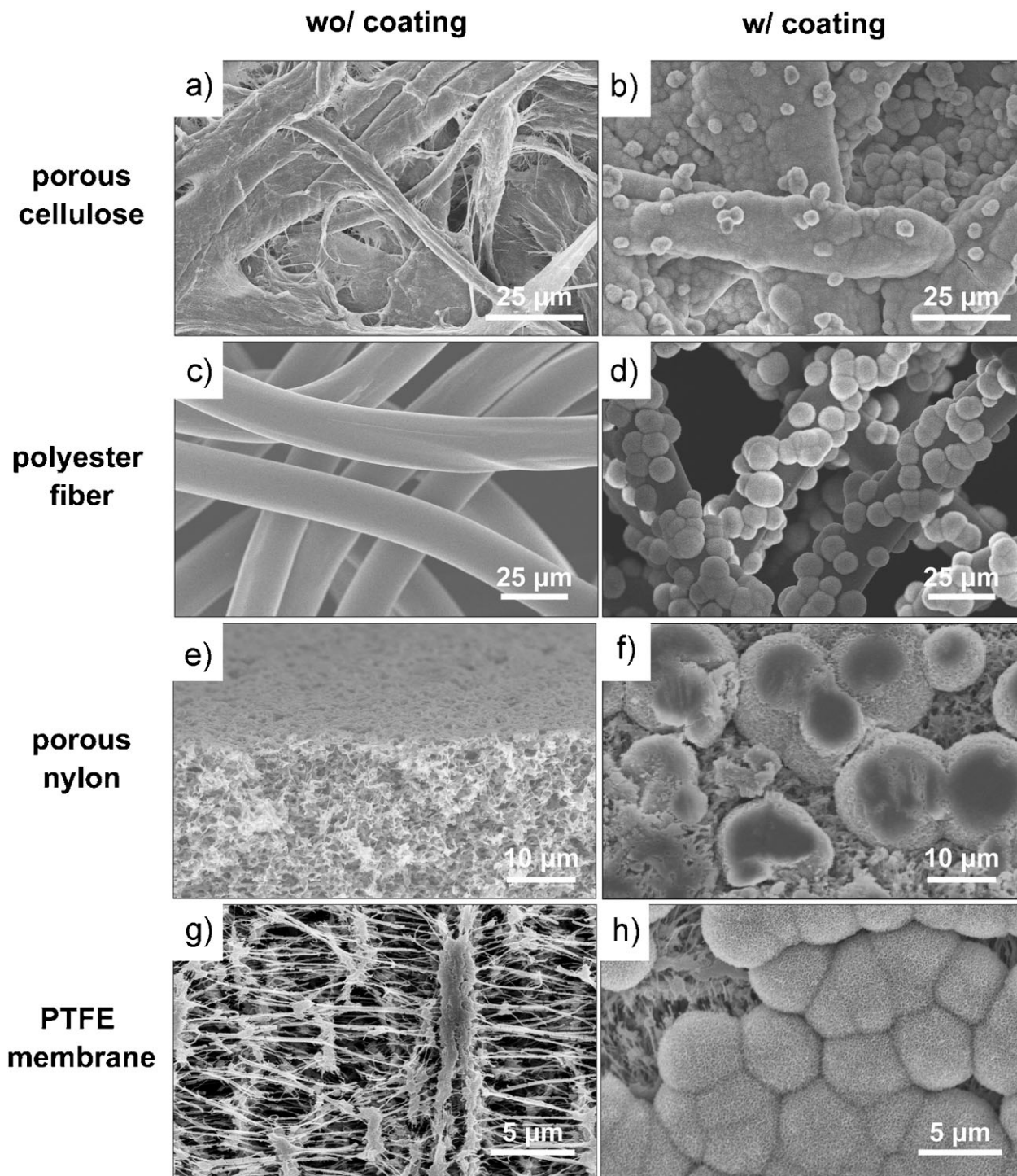
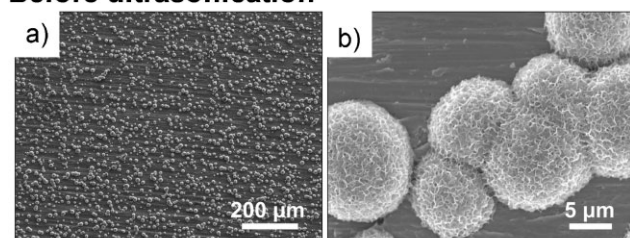


Figure 7. The fabrication of organic–inorganic hybrid materials via pHAF. The SEM images demonstrate that the hydroxyapatite crystals can be integrated into 3D porous materials in a material-independent manner. The tested 3D materials of porous cellulose, polyester fiber, porous nylon, and PTFE membrane were hybridized with hydroxyapatites. All the materials were incubated in $1.5\times$ SBF for 2 days at 37°C after polydopamine treatment.

Characterization: The morphological changes after biomineralization were investigated with an S-4800 field-emission scanning electron microscope (Hitachi High-technologies Co., Japan) and a Tecnai F20 transmission electron microscope (FEI Company, OR, USA) at an

acceleration voltage of 10 kV and 200 kV, respectively. For TEM analysis, hydroxyapatite was transferred onto a carbon/formvar-coated Cu TEM grid by carefully rubbing the grid with hydroxyapatite-formed substrates. For selected-area electron diffraction (SAED) analysis, hydroxyapatite minerals

Before ultrasonication



After ultrasonication

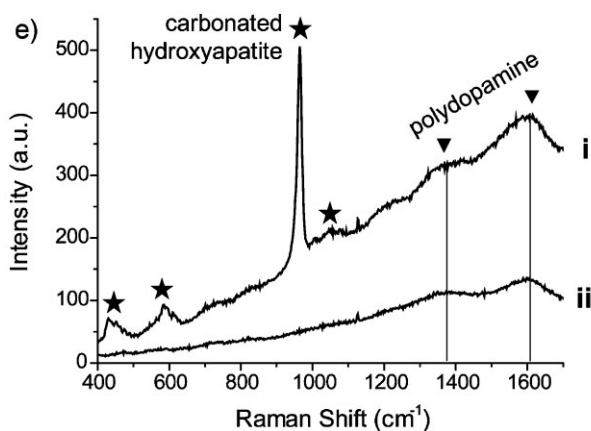
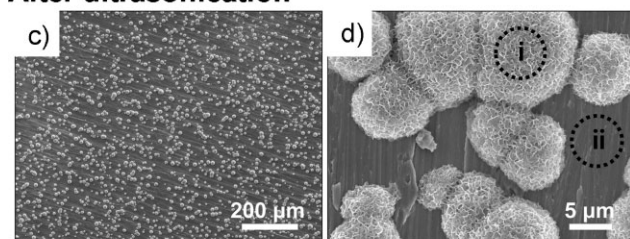


Figure 8. Adhesion stability of the polydopamine layer and hydroxyapatite minerals grown by pHAF onto a Ti substrate. Polydopamine-modified Ti substrates were incubated in $1.5 \times$ SBF for 2 days at 37°C , and were then investigated by a–d) electron microscopy and e) micro-Raman spectroscopy before (a,b) and after (c–e) exposure to ultrasonication (Branson 5510R-DTH, 42 kHz, 135 W) in a water bath. Both the hydroxyapatite minerals (i) and the polydopamine film (ii) were still firmly attached to the underlying Ti substrate even after ultrasonication for 1 h.

were grown on a Si wafer using pHAF, and the diffraction patterns of the hydroxyapatite crystals were measured using a D/MAX-RC thin-film X-ray diffractometer (Rigaku Co., Japan) under the following conditions: scan speed, 3°min^{-1} ; Cu $K\alpha$ radiation, $\lambda = 1.5418 \text{ \AA}$; scan range, 4° – 50° . The formation of hydroxyapatite was also investigated with a LabRAM HR UV–vis–NIR high-resolution dispersive Raman microscope (Horiba Jobin Yvon, France). The Raman spectra were obtained by accumulating 60 scans with a resolution of 4 cm^{-1} in the spectral range of 100 – 1900 cm^{-1} .

Preosteoblast Culture and Viability Assay: Mouse preosteoblasts (MC3T3-E1) were cultured in a modified Eagle's minimal essential medium (α -MEM, Welgene, Korea) with 10% fetal bovine serum (FBS, Welgene, Korea) and 1% antibiotics (Invitrogen, Carlsbad, CA, USA). Cells were seeded at a density of 1×10^4 cells per well and cultured for 2 days. The cell viability was determined using a 3-[4,5-dimethylthiazol-2-yl]-2,5-diphenyl tetrazolium bromide (MTT) assay. $50 \mu\text{L}$ of the MTT solution (5 mg mL^{-1} in phosphate buffered saline (PBS)) was added to each well, and the cells were incubated additionally for 3 h at 37°C . The resulting formazan crystals were dissolved in dimethylsulfoxide, and the absorbance

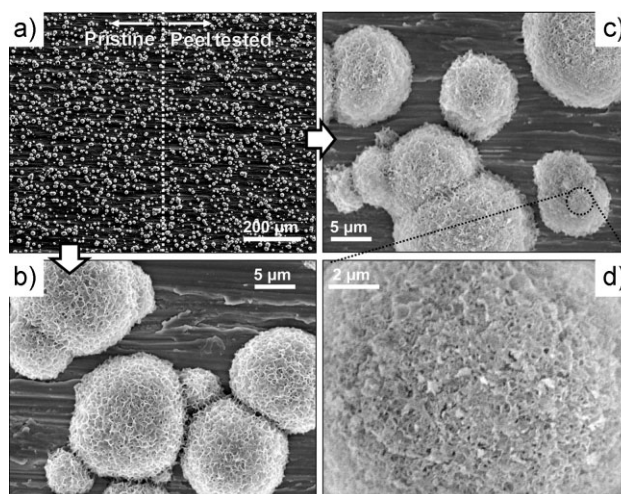


Figure 9. Electron microscopy images of hydroxyapatite minerals grown on Ti substrate by pHAF after the peeling test. The samples were prepared by modifying the Ti substrates with a polydopamine coating and incubating in $1.5 \times$ SBF for 2 days at 37°C (a,b). A peeling test was carried out by pressing a piece of Scotch tape (KS T1046, adhesive strength higher than 1.23 N cm^{-1}) down firmly on the samples and removing it quickly. Although a slight disruption of the lath-like structure of the hydroxyapatite minerals was observed after the peeling test (c,d), about 85% of hydroxyapatite minerals remained attached to the underlying Ti substrate.

was measured at 595 nm using a Victor3 microplate reader (Perkin Elmer Inc., Waltham, MA, USA). The cell morphology was observed by staining the actin filaments and nucleus. The cells were fixed by 3.7% formaldehyde and then permeabilized using 0.1% Triton X-100. Rhodamine-phalloidin (Invitrogen, Carlsbad, CA) and Hoechst 33258 (Sigma-Aldrich, St. Louis, MO) were used for staining of the actin filament and nucleus, respectively.

Acknowledgements

This study was supported by the institutional grant from KAIST Institute for the NanoCentury (KINC) and the National Research Foundation (NRF) via the National Research Laboratory (R0A-2008-000-20041-0; C.B.P.), Engineering Research Center (2008-0062205; C.B.P.), Converging Research Center (2009-0082276; C.B.P.), and Molecular-Level Interface Research Center (2010-0001954, H.L.) of the Republic of Korea. This research was also partially supported by the Fundamental R&D Program for Core Technology of Materials from the Ministry of Knowledge Economy of the Republic of Korea. Supporting information is available online from Wiley Interscience or from the author.

Received: December 14, 2009

Revised: March 14, 2010

Published online: May 25, 2010

- [1] a) S. Mann, *J. Mater. Chem.* **1995**, *5*, 935. b) S. Mann, *Biomaterialization: Principles and Concepts in Bioinorganic Materials Chemistry*, Oxford University Press, Oxford, New York, NJ **2001**, Ch. 6. c) R. Langer, J. P. Vacanti, *Science* **1993**, *260*, 920. d) R. Langer, D. A. Tirrell, *Nature* **2004**, *428*, 487–492. e) P. Fratzl, R. Weinkamer, *Prog. Mater. Sci.* **2007**, *52*, 1263.
- [2] a) S. Weiner, H. D. Wagner, *Annu. Rev. Mater. Sci.* **1998**, *28*, 271. b) T. A. Taton, *Nature* **2001**, *412*, 491.
- [3] A. George, A. Veis, *Chem. Rev.* **2008**, *108*, 4670.
- [4] a) J. Song, E. Saiz, C. R. Bertozzi, *J. Am. Chem. Soc.* **2003**, *125*, 1236. b) G. He, T. Dahl, A. Veis, A. George, *Nat. Mater.* **2003**, *2*, 552.

- c) W. L. Murphy, D. J. Mooney, *J. Am. Chem. Soc.* **2002**, 124, 1910.
d) L. T. De Jonge, S. C. G. Leeuwenburgh, J. J. P. van den Beucken, J. G. C. Wolke, J. A. Jansen, *Adv. Funct. Mater.* **2009**, 19, 755.
e) E. D. Spoerke, S. G. Anthony, S. I. Stupp, *Adv. Mater.* **2009**, 21, 425.
f) J. Song, V. Malathong, C. R. Bertozzi, *J. Am. Chem. Soc.* **2005**, 127, 3366.
g) M. Kikuchi, S. Itoh, S. Ichinose, K. Shinomiya, J. Tanaka, *Biomaterials* **2001**, 22, 1705. h) M. J. Olszta, X. Cheng, S. S. Jee, R. Kumar, Y.-Y. Kim, M. J. Kaufman, E. P. Douglas, L. B. Gower, *Mater. Sci. Eng.* **2007**, 58, 77.
i) Y. Leng, J. Chen, S. Qu, *Biomaterials* **2003**, 24, 2125.
- [5] a) L. L. Hench, *Biomaterials* **1998**, 19, 1419. b) R. Z. LeGeros, *Chem. Rev.* **2008**, 108, 4742.
- [6] a) H. Lee, S. M. Dellatore, W. M. Miller, P. B. Messersmith, *Science* **2007**, 318, 426. b) H. Lee, J. Rho, P. B. Messersmith, *Adv. Mater.* **2009**, 21, 431.
c) Y. Fu, P. Li, Q. Xie, X. Xu, L. Lei, C. Chen, C. Zou, W. Deng, S. Yao, *Adv. Funct. Mater.* **2009**, 19, 1784. d) A. Postma, Y. Yan, Y. Wang, A. N. Zelikin, E. Tjijto, F. Caruso, *Chem. Mater.* **2009**, 21, 3042. e) R. Ouyang, J. Lei, H. Ju, *Chem. Commun.* **2008**, 5761. f) F. Bernsmann, L. Richert, B. Senger, P. Lavalle, J.-C. Voegel, P. Schaaf, V. Ball, *Soft Matter* **2008**, 4, 1621.
g) B. Li, W. Liu, Z. Jiang, X. Dong, B. Wang, Y. Zhong, *Langmuir* **2009**, 25, 7368. h) S. Chen, Y. Chen, Y. Lei, Y. Yin, *Electrochem. Commun.* **2009**, 11, 1675. i) J. Ou, J. Wang, S. Liu, J. Zhou, S. Ren, S. Yang, *Appl. Surf. Sci.* **2009**, 256, 894. j) H. Lee, N. F. Scherer, P. B. Messersmith, *Proc. Natl. Acad. Sci. USA* **2006**, 103, 12 999.
- [7] a) C. Ohtsuki, H. Kushitani, T. Kokubo, S. Kotani, T. Yamamuro, *J. Biomed. Mater. Res.* **1991**, 25, 1363. b) M. Tanahashi, T. Yao, T. Kokubo, M. Minoda, T. Miyamoto, T. Nakamura, T. Yamamuro, *J. Am. Ceram. Soc.* **1994**, 77, 2805.
- [8] a) S. W. Taylor, D. B. Chase, M. H. Emptage, M. J. Nelson, J. H. Waite, *Inorg. Chem.* **1996**, 35, 7572. b) N. Holten-Anderson, T. E. Mates, M. S. Toprak, G. D. Stucky, F. W. Zok, J. H. Waite, *Langmuir* **2009**, 25, 3323.
c) W. M. Chirdon, W. J. O'Brian, R. E. Robertson, *J. Biomed. Mater. Res. Part B* **2003**, 66B, 532.
- [9] M. Geetha, A. K. Singh, R. Asokamani, A. K. Gogia, *Prog. Mater. Sci.* **2009**, 54, 397.
- [10] a) M. Ohring, *Materials Science of Thin Films: Deposition & Structure*, 2nd ed. Academic Press San Diego, CA **2002**, Ch. 7. b) J. Nourmohammadi, S. K. Sadrnezhad, A. B. Ghader, *J. Mater. Sci. – Mater. Med.* **2008**, 19, 3507.
- [11] B. Fei, B. Qian, Z. Yang, R. Wang, W. C. Liu, C. L. Mak, J. H. Xin, *Carbon* **2008**, 46, 1795.
- [12] a) A. Antonakos, E. Liarokapis, T. Leventouri, *Biomaterials* **2007**, 28, 3043.
b) G. Wei, J. Reichert, J. Bossert, K. D. Jandt, *Biomacromolecules* **2009**, 9, 3258.
- [13] Y. Lee, Y. M. Hahm, S. Matsuya, M. Nakagawa, K. Ishikawa, *J. Mater. Sci.* **2007**, 42, 7843.
- [14] S. H. Ku, J. Ryu, S. K. Hong, H. Lee, C. B. Park, *Biomaterials* **2010**, 31, 2535.